PHYSICAL REVIEW LETTERS

Effective Long-Range Attraction between Protein Molecules in Solutions Studied by Small Angle Neutron Scattering

Yun Liu,[1] Emiliano Fratini,[2] Piero Baglioni,[1,2] Wei-Ren Chen,[1] and Sow-Hsin Chen[1,*]

[1]*Department of Nuclear Engineering, Massachusetts Institute of Technology, Cambridge, Massachusetts 02139, USA*
[2]*Department of Chemistry and CSGI, University of Florence, via della Lastruccia 3, 50019 Florence, Italy*
(Received 8 February 2005; published 8 September 2005)

Small angle neutron scattering intensity distributions taken from cytochrome C and lysozyme protein solutions show a rising intensity at a very small wave vector Q, which can be interpreted in terms of the presence of a weak long-range attraction between protein molecules. This interaction has a range several times that of the diameter of the protein molecule, much greater than the range of the screened electrostatic repulsion. We show evidence that this long-range attraction is closely related to the type of anion present and ion concentration in the solution.

PACS numbers: 87.14.Ee, 61.12.Ex, 82.35.Rs

The bottleneck of protein crystallography is the lack of systematic methods to obtain protein crystals. This is partly due to incomplete understanding of the physical chemistry conditions controlling the growth of protein crystals. A full comprehension of the effective protein interactions and phase behavior is therefore essential. It has been shown that the crystallization curves of some globular proteins appear to coincide with the phase diagrams of a hard sphere system interacting with a short-range attraction [1–3]. Small angle neutron and x-ray scattering investigations of proteins suggest the presence of a short-range attractive interaction between protein molecules besides the electrostatic repulsion induced by the residual charges [4–6]. The Derjaguin-Landau-Verwey-Overbeek (DLVO) potential has been successfully applied to many colloidal systems and protein solutions [3,4]. However, it does not seem to fully explain the rich behavior of proteins [4,7–9], and due to the complexity of these systems (anisotropic property, irregular shape, distributed charge patches, etc.), a complete understanding of the properties of the effective interactions between protein molecules in solutions remains a challenge [8].

Recent measurements of small angle neutron scattering (SANS) intensity distribution in protein solutions show interesting results [5,6,10]. Beside the normal first diffraction peak, it is present a peak (cluster peak) appearing at a much smaller scattering wave vector, Q, due to the formation of ordered clusters. The appearance of a cluster peak is explained as due to the competition of a short-range attraction and a long-range electrostatic repulsion [5,11,12]. Moreover, a rising intensity as Q approaches zero (zero-Q peak) is observed in both liquidlike and solidlike samples, which implies that the effective potential should have more features in addition to the well known short-range attraction and electrostatic repulsion. The existence of a long-range attraction between protein molecules has already been postulated in theoretical studies. Noro *et al.* suggested that the presence of a long-range attractive force between protein molecules should

shift the metastable fluid-fluid critical point out of gel regime [13]. Thus a protein crystallization may occur without gelation. By employing two-Yukawa potential model, Lawlor *et al.* showed that the introduction of a long-range attraction between protein molecules can enhance crystal growth by avoiding the formation of a disordered state, an attractive glass [14,15], while preserving the equilibrium features of a system with the short-range attraction [16].

In this Letter, by systematically studying the zero-Q peak, we find that a weak long-range attraction needs to be considered to explain the SANS scattering intensity distributions. The properties of this long-range attraction potential are also investigated. Cytochrome C from horse heart (Product No. C7752) was purchased from Sigma and is obtained using a procedure that avoids the trichloroacetic acid (TCA) that is known to promote the dimer formation. Cytochrome C has been dialyzed 3 times in order to remove any extra salt. Buffers are not used to avoid possible bindings of organic molecules to the protein surface. Lysozyme from chicken egg white was purchased from Fluka (Product No. L7651) and used without further purification. The pD of cytochrome solutions at 7.2 and 9.5 has been adjusted by a HCl standard solution. Only samples of lysozyme have been prepared in 20 mM 4-(2-hydroxyethyl)-1-piperazine-ethanesulphonic acid (HEPES) buffer. The pD value was sequentially checked by an ISFET pHMeter (KS723) before and after each performed experiment and found stable within ± 0.1 units. All samples were prepared a few days before the scheduled experiments to allow the hydrogen/deuterium exchange. For all solutions the final protein concentration has been measured by UV-visible spectroscopy. Our experiments were performed at the small angle neutron scattering station, NG7, at the Center of Neutron Research in the National Institute of Standard and Technology. Two configurations have been used to reach a wide range of the wave vector, Q, from 0.004 Å^{-1} to 0.30 Å^{-1}, where $Q = \frac{4\pi}{\lambda} \sin(\theta/2)$, λ is the neutron wavelength, θ the neutron

scattering angle. All the analyses have taken into account the instrumental resolution correction.

SANS intensity distribution, $I(Q)$, can be expressed as $I(Q) = A\bar{P}(Q)S(Q)$, where $\bar{P}(Q)$ is the normalized particle structure factor, $S(Q)$ the interparticle structure factor, and A the known amplitude factor which is proportional to the volume fraction and the square of the neutron scattering length contrast between protein and solvent [17]. Cytochrome C has an ellipsoidal shape with the semimajor and minor axes, $a \times b \times b = 15 \times 17 \times 17$ Å^3, while a lysozyme molecule has a dimension $a \times b \times b = 22.5 \times 15 \times 15$ Å^3. $\bar{P}(Q)$ is calculated by considering the ellipsoidal shape of the protein. $S(Q)$ is calculated by solving the Ornstein-Zernike (OZ) equation within the mean spherical approximation (MSA) closure involving an effective pair potential, $V(r)$, to be specified later. The effect on $S(Q)$ due to the nonspherical shape of a particle is approximately taken into account by using the decoupling approximation [18].

Figure 1 shows theoretical calculations together with the SANS result from a cytchrome C solution at $pD = 11$ with 1% volume fraction in 1 M NaCl in the inset. Conventionally, the effective interprotein potential is considered to consist of a short-range attractive and a long-range electrostatic repulsive part. The repulsion is screened out by the concentrated salt. Therefore, $S(Q)$ could be obtained by solving OZ equation by considering only a short-range attraction, which can be approximated by an attractive potential of a Yukawa form [19], $V(r) = -K\frac{e^{-Z(r-1)}}{r}$, where K is normalized by k_BT, and r is the interprotein distance normalized by σ with $\sigma = 2(ab^2)^{1/3}$. The interaction range, $\frac{1}{Z}$, is approximately about 10% of the protein diameter [4]. Figure 1(a) shows the theoretically calculated SANS intensity distribution with $Z = 10$ by taking the amplitude factor A equal to unity. As K

increases from 0.5 to 16, the intensity at $Q = 0$ increases gradually. The results from a short-range attraction always smoothly change the whole scattering curve and cannot reproduce the sharp rising up of experimental SANS intensity at very low Q (zero-Q peak) as shown in the inset. Since the typical strength of short-range attraction is smaller than $10k_BT$ [4,20,21], the short-range attraction cannot explain the observed SANS intensity distribution. In Fig. 1(b), K is fixed at 0.5. When Z decreases from 10 to 0.5, i.e., the attraction range increases, the intensity at low Q increases sharply and the theoretical curve exhibits a similar trend to the experimental intensity. The comparison between the experimental result and theoretical curves thus suggests that the zero-Q peak could be induced by a weak long-range attraction. Therefore, the effective potential between protein molecules in solutions should consist of three features: a short-range attraction, an intermediate-range electrostatic repulsion, and a weak long-range attraction. This zero-Q peak has been overlooked in previous experiments due to the limited Q range covered [17]. However, it has been observed before in lysozyme protein solutions [22] and was explained as due to the long-range density fluctuation.

To investigate the properties of this long-range attraction, three different cytochrome C samples at $pD = 11$ with 1% volume fraction added with different salts were measured and their SANS intensity distributions with error bars are plotted in semilog scale to clearly show zero-Q peaks in Fig. 2. The salt concentration, which is indicated in the figure, has been changed to keep the same ionic strength. Very interestingly, the results show that the zero-Q peak depends on the different anions added. NaCl induces a much weaker zero-Q peak compared with that of NaSCN and Na$_2$SO$_4$. Since the true form of this long-range attraction is still unknown, in order to fit the experimental results, we assume that the effective interprotein potential
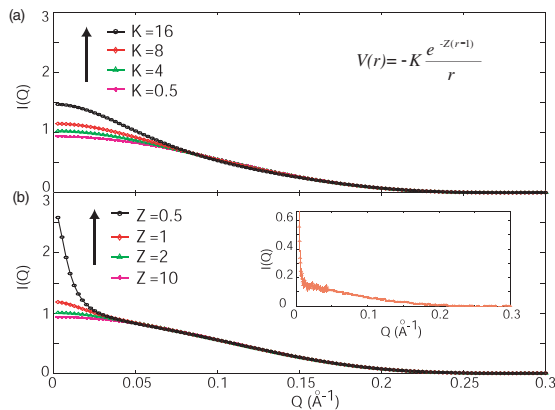
FIG. 1 (color online). Theoretical calculations of $I(Q)$ resulting from one Yukawa attraction at 1% volume fraction. (a) The effect due to the variation of the attraction strength, K, at $Z = 10$. (b) The effect due to the variation of the attraction range, $1/Z$, at $K = 0.5$. The inset shows $I(Q)$ from a cytochrome C sample at 1% volume fraction in 1 M NaCl at $pD = 11$.
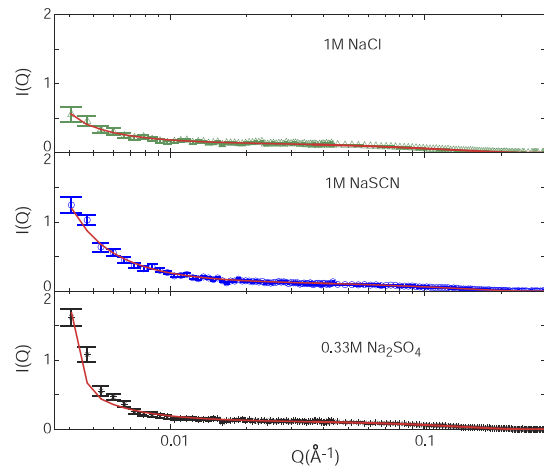
FIG. 2 (color online). SANS intensity distribution of cytochrome C solutions at $pD = 11$ and at 1% volume fraction with different salts added. The solid lines are the theoretical analyses.

TABLE I. Fitted parameters using the two attractive Yukawa form potential. Results are shown in Fig. 2.

	a(Å)	K_1	Z_1	K_2	Z_2
NaCl	14.7	7 ± 3	7 ± 3	0.11 ± 0.02	0.20 ± 0.01
NaSCN	14.6	8 ± 5	10 ± 6	0.33 ± 0.02	0.35 ± 0.01
Na$_2$SO$_4$	14.7	4 ± 5	10 ± 10	0.24 ± 0.02	0.27 ± 0.02

can be simulated by two attractive Yukawa form potential, $V_{TY}(r) = -K_1 \frac{e^{-Z_1(r-1)}}{r} - K_2 \frac{e^{-Z_2(r-1)}}{r}$. The first term is used to simulate the short-range attraction, while the other one is used to simulate the long-range attraction. The fitted results are given in Table I.

The fitting is not sensitive at all to the short-range attraction. The long-range attraction has a weak strength (less than $0.5k_BT$) and a range of 3–5 times the protein diameter, and it is very sensitive to the anions added to the solutions. This implies that the long-range attraction is at least partly induced by the ion cloud around protein molecules. Depletion forces and van der Waals force cannot explain this feature. It is very interesting to notice that the strength and range of the long-range attraction is about the same value as the attractive potential between like-charged particles [23]. However, a charged colloidal particle typically has a uniform charge distribution on the surface, while a protein molecule has both positive and negative charge patches, which make the ion cloud distribution around a protein much more complicated.

Since the long-range attraction seems to be induced by the ion cloud, if we can minimize the ion concentration in solutions, we should expect to greatly suppress the zero-Q peak. Figure 3 shows SANS results of two cytochrome C samples at $pD = 7.2$ and $pD = 9.5$ with 5% volume fraction. Without adding any extra salt in solutions, the ion concentration is determined by the dissociated charges from proteins. The cytochrome C molecule has a much smaller charge number at $pD = 9.5$ than that at $pD = 7.2$, being the isoelectric point, pI, about 10.2. This leads to a smaller ion concentration in solutions at $pD = 9.5$.
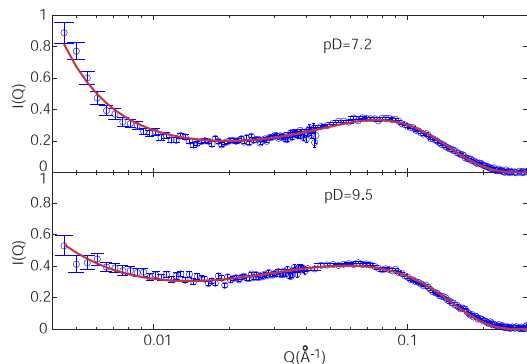

FIG. 3 (color online). SANS intensity distributions of cytochrome C samples at 5% volume fraction. The solid lines are theoretical analyses using two-Yukawa potential.

Correspondingly, the SANS intensity distribution shows a zero-Q peak weaker than that at $pD = 7.2$. This implies that the zero-Q peak depends on the ion concentrations, and is not likely due to permanent cluster formations, since a weaker repulsion should favor larger cluster formations and thus induce larger zero-Q peak at $pD = 9.5$, which is in contrast with our experimental results. In order to quantitatively analyze the zero-Q peak, we again used the two-Yukawa potential model. However, due to the existence of the weak long-range attraction, we need three Yukawa terms to completely simulate the features of the potential. We argue that in cytochrome C solutions, the short-range attraction is small so that its effect on the structure factor should be very small at the relatively low volume fraction. Actually, the first diffraction peak of SANS intensity distribution in cytochrome C solutions has been successfully analyzed by only considering the electrostatic repulsion at various pD values [12,17]. Furthermore, for cytochrome C solutions, we did not observe the cluster peak as it is observed for lysozyme solutions. The lack of cluster peak is attributed to the weak short-range attraction. Therefore, we ignore the short-range attraction and we use the second term of V_{TY} for the long-range attraction contribution and the first term of V_{TY} to simulate the electrostatic repulsion, which can be calculated by the charge number of the protein molecule and the ionic strength [12,17]. The fitted results given in Table II show that the range of the long-range attraction is about 3–5 times of protein diameter, and also confirm our direct observation from Fig. 3; i.e., the strength of long-range attraction at $pD = 9.5$ is much smaller.

After showing the existence of the long-range attraction in solutions dominated by monomers, it is important to check its existence in protein solutions having equilibrium clusters. Figure 4 shows the results of lysozyme protein solutions at $pD = 5.1$ and at 10% and 20% volume fraction in HEPES buffer. The top panel shows SANS intensity distributions with the fitted results and the bottom panel shows the calculated $S(Q)$ from the fitted parameters. The *main peak* in the top panel is a cluster peak as it is independent of volume fraction. Interestingly, even in the presence of cluster peak, both results have shown the zero-Q peak, which was overlooked by previous experiments [5]. The coexistence of the cluster peak and zero-Q peak clearly indicates the necessity of introducing a third potential feature, a long-range attraction. We used the two-Yukawa model previously described to fit the main peak, assuming that the first term is the short-range attraction and the second term the electrostatic repulsion. The fitted

TABLE II. Fitted parameters obtained using the two-Yukawa potential. Results are shown in Fig. 3.

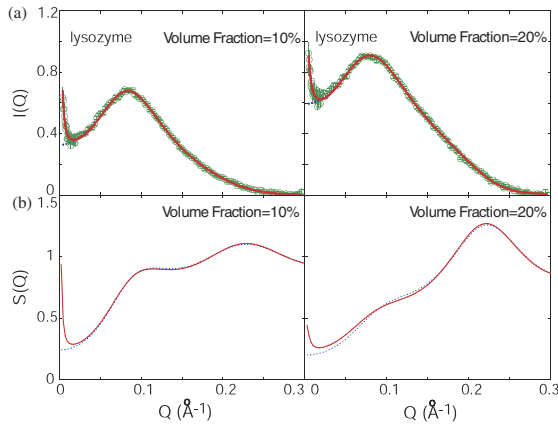|	a(Å)	Charge Number	K_2	Z_2
$pD = 7.2$	15.3	3.8 ± 0.1	0.37 ± 0.02	0.34 ± 0.01
$pD = 9.5$	15.4	1.7 ± 0.1	0.08 ± 0.01	0.21 ± 0.01

FIG. 4 (color online). SANS intensity distributions of lyso-zyme samples at $pD = 5.1$ with 20 mM HEPES buffer. Dotted lines (a) and (b) are fitted by considering only a short-range attraction and electrostatic repulsion. Solid lines (a) and (b) are the fitted results by using three Yukawa form potential. Lower panel shows the calculated structure factor, $S(Q)$.

TABLE III.   Fitted parameters from fitting the cluster peaks by using only a short-range attraction and the electrostatic repulsion (see Fig. 4).

	$a(\text{Å})$	Charge Number	K_1	Z_1
10%	21.1	7.0 ± 1.2	6.9 ± 1.0	14 ± 5
20%	21.2	6.8 ± 1.5	7.7 ± 1.2	15 ± 5

saturated protein solutions may be induced by the long-range attraction [28,29].

curves are shown as dotted lines in the figure and the fitting results are given in Table III. The attraction strength is about $7k_BT$ with 7% of attraction range, which is consis-tent with Ref. [3]. In order to fit the complete SANS distribution, we use the two-Yukawa model as the refer-ence system and treat the long-range attraction as a pertur-bation by employing the random phase approximation [24]. The long-range attraction is considered here as a third Yukawa form, $-K_3 \frac{e^{-Z_3(r-1)}}{r}$. The results fitted with this approximation are shown as solid line. The addition of this third potential feature slightly changes the previous fitting parameters. The parameters for the long-range at-traction are $K_3 = 0.038 \pm 0.005$ and $Z_3 = 0.17 \pm 0.01$ for the 10% lysozyme sample, while for the 20% sample, $K_3 = 0.019 \pm 0.002$ and $Z_3 = 0.21 \pm 0.03$.

Judging from SANS results on both cytochrome C and lysozyme protein solutions, we believe that the existence of weak long-range attraction is universal for all protein solutions. Its strength and range depend both on the type of anion and ion concentration in solutions. In other words, it depends on the ion cloud around protein molecules. Our finding has important implications in understanding the protein crystallization process. There are numerous mea-surements of a second virial coefficient in protein solutions by static light scattering experiments [25,26]. Because of the very small Q range the light scattering can access, its intensity is closely related to the height of the zero-Q peak, which depends on the feature of the long-range attraction. Thus we believe that the conclusions derived from those observations should take into account the existence of the weak long-range attraction. The charge dependence of some of these phenomena can then be naturally related to the charge dependence of the long-range attraction [8,27]. Also the very large cluster formation or gelation in super-

[1] D. Rosenbaum *et al.*, Phys. Rev. Lett. **76**, 150 (1996).
[2] M. H. J. Hagen *et al.*, J. Chem. Phys. **101**, 4093 (1994).
[3] G. Pellicane *et al.*, J. Phys. Condens. Matter **16**, S4923 (2004).
[4] A. Tardieu *et al.*, J. Cryst. Growth **196**, 193 (1999).
[5] A. Stradner *et al.*, Nature (London) **432**, 492 (2004).
[6] B. Lonetti *et al.*, Phys. Chem. Chem. Phys. **6**, 1388 (2004).
[7] M. L. Broide *et al.*, Phys. Rev. E **53**, 6325 (1996).
[8] R. Piazza, Curr. Opin. Colloid Interface Sci. **8**, 515 (2004).
[9] A. Striolo *et al.*, J. Chem. Phys. **116**, 7733 (2002).
[10] P. Baglioni *et al.*, J. Phys. Condens. Matter **16**, S5003 (2004).
[11] F. Sciortino *et al.*, Phys. Rev. Lett. **93**, 055701 (2004).
[12] Y. Liu *et al.*, J. Chem. Phys. **122**, 044507 (2005).
[13] M. G. Noro *et al.*, Europhys. Lett. **48**, 332 (1999).
[14] K. Dawson *et al.*, Phys. Rev. E **63**, 011401 (2001).
[15] S. H. Chen *et al.*, Science **300**, 619 (2003).
[16] A. Lawlor *et al.*, Prog. Colloid Polym. Sci. **123**, 104 (2004).
[17] C. F. Wu *et al.*, J. Chem. Phys. **87**, 6199 (1987).
[18] M. Kotlarchyk *et al.*, J. Chem. Phys. **79**, 2461 (1983).
[19] M. Malfois *et al.*, J. Chem. Phys. **105**, 3290 (1996).
[20] W. Eberstein *et al.*, J. Cryst. Growth **143**, 71 (1994).
[21] J. Z. Xia *et al.*, Biophys. J. **66**, 861 (1994).
[22] R. Giordano *et al.*, Phys. Rev. A **43**, 6894 (1991).
[23] G. M. Kepler *et al.*, Phys. Rev. Lett. **73**, 356 (1994); Y. Han *et al.*, Phys. Rev. Lett. **91**, 038302 (2003).
[24] K. Shukla and R. Rajagopalan, Colloids Surf. A **81**, 181 (1993).
[25] A. George and W. W. Wilson, Acta Cryst. D **50**, 361 (1994).
[26] O. D. Velev *et al.*, Biophys. J. **75**, 2682 (1998).
[27] M. Muschol *et al.*, J. Chem. Phys. **103**, 10424 (1995).
[28] M. Sokuri *et al.*, FEBS Lett. **295**, 84 (1991).
[29] N. Niimura *et al.*, J. Cryst. Growth **154**, 136 (1995).